Title

Using model reduction to predict the soil surface C1800 flux: An example of representing complex biogeochemical dynamics in a computationally efficient manner

Author

Riley, W.J.

Publication Date

2012-10-01

DOI

DOI:10.5194/gmdd-5-3469-2012

Peer reviewed

Using model reduction to predict the soil-surface $C^{18}OO$ flux: an example of representing complex biogeochemical dynamics in a computationally efficient manner

W. J. Riley

Earth Sciences Division, Lawrence Berkeley National Laboratory, Bldg 84-1134,
1 Cyclotron Road, Berkeley, California 94720, USA

tationally tractable manner. δF_s depends on the $\delta^{18}O$ value of soil water, soil moisture, soil temperature, and soil CO_2 production (all of which are depth-dependent), and the $\delta^{18}O$ value of above-surface CO_2. We tested the HDMR approach over a growing season in a C_4-dominated pasture using two vertical soil discretizations. The difference between the HDMR approach and the full model solution in the three-month integrated isoflux was less than 0.2 % (0.5 mol m^{-2} ‰), and the approach is up to 100 times faster than the full numerical solution. This type of model reduction approach allows representation of complex coupled biogeochemical processes in regional and global climate models and can be extended to characterize subgrid-scale spatial heterogeneity.

1 Introduction

Atmospheric CO_2 has substantial impacts on global climate, both over the long-term and, as we have witnessed since the beginning of the industrial revolution, much shorter time scales (Watson et al., 2001). As a result, the impacts of anthropogenic CO_2 emissions and climate system feedbacks on the long-term state and stability of the climate are currently the focus of much research. Since interactions with the terrestrial biosphere dominate spatial and inter- and intra-annual variations in atmospheric CO_2 concentrations (Tans et al., 1990), developing reliable models of ecosystem CO_2 exchanges is necessary to predict future climate.

Terrestrial carbon cycle models used at the site and regional scales and in Earth System Models (ESMs; e.g., Bonan et al., 2002; Denning et al., 1996; Parton et al., known to exist at scales substantially finer than those represented in current ESMs ($\sim$ 100 km resolution; King et al., 2010; Thompson et al., 2011), either explicitly or by integrating scaling rules based on mechanistic process representation.

Land models are often tested and calibrated against field eddy covariance measurements of net CO_2 ecosystem exchange (NEE) (Baldocchi et al., 2001). Difficulties in interpreting these NEE measurements arise from landscape horizontal and vertical heterogeneity, footprint uncertainty, unsteady conditions, and stable nocturnal conditions (Aubinet et al., 2000; Baldocchi, 2003; Goulden et al., 1996). Further, ecosystem model development requires accurate estimates of the gross CO_2 fluxes comprising the net flux, i.e., the assimilated (photosynthetic) and respired fluxes. This partitioning is necessary since the processes controlling these fluxes respond differently to environmental forcings and therefore require separate model formulations and parameterizations.

Measurements of the stable isotope ^{18}O in CO_2 have been proposed as a tracer to partition measured net CO_2 fluxes into component gross fluxes (Yakir and Wang, 1996), identify regional distributions of CO_2 exchanges (Ciais et al., 1997a,b; Cuntz et al., 2003; Francey and Tans, 1987; Peylin et al., 1999), and investigate interactions between the C and water cycles (Buenning et al., 2012; Wingate et al., 2009). However, using measurements of ^{18}O in CO_2 for these methods requires accurate estimation of the $\delta^{18}O$ value of the soil-surface CO_2 flux (δF_s (‰)), which depends on a complex suite of interactions between the C and water cycles (Riley et al., 2002; Tans, 1998). Using this example, we illustrate here a computationally efficient approach to represent these dynamics in a manner appropriate for inclusion in regional and global models.

phase can substantially change the $\delta^{18}O$ value of the soil gas CO_2. Upon dissolution, CO_2 can exchange ^{18}O atoms with the water, thereby acquiring the ^{18}O composition of the water. The impact of this exchange on the $\delta^{18}O$ value of soil water (δ_{sw} (‰)) is small, since there are orders of magnitude more H_2O than CO_2 molecules in soil moisture. The competition between CO_2 diffusion through the open pore space and dissolution into the soil water can substantially impact δF_s (Miller et al., 1999; Riley, 2005).

Three classes of methods to estimate δF_s have been reported. Several authors have hypothesized that a depth-integrated $\delta^{18}O$ value of soil water and a constant effective kinetic fractionation factor can be used (Ciais et al., 1997a,b; Miller et al., 1999; Yakir and Wang, 1996). Tans (1998) developed steady-state analytical solutions for δF_s, which Stern et al. (2001) applied to study the impact of invasion fluxes on the net surface $C^{18}OO$ exchange. Finally, numerical modeling approaches have been developed to account for transient conditions and gradients in the $\delta^{18}O$ value of the various water pools impacting δF_s (e.g., ISOLSM, Riley et al., 2002; Stern et al., 1999).

ISOLSM has been integrated with the general circulation model CCM3 (Buenning et al., 2012) to investigate the impact of ecosystems on the $\delta^{18}O$ value of atmospheric CO_2 (δ_a). However, the soil-gas diffusion and reaction submodels in ISOLSM are computationally expensive. The High-Dimensional Model Representation (HDMR) method applied here allows reduction of the full model to a series of look up tables, while still characterizing second order interactions between variables important in the system. This approach substantially reduces simulation runtime (by up to a factor of 100), while still generating accurate δF_s predictions.

2 Methods

2.1 Estimating δF_s using ISOLSM

ISOLSM integrates modules that simulate ^{18}O ecosystem exchanges in H_2O and CO_2 with the land-surface model LSM1 (Bonan, 1996). LSM1 is a "big-leaf" model that calculates internally consistent ecosystem energy, CO_2, and H_2O exchanges with the atmosphere. Soil moisture, advective water fluxes, and temperature, all of which impact δ_{sw}, are calculated at user-defined depths in the soil.

The isotopic mechanisms integrated in ISOLSM are described in detail by Riley et al. (2002); the model has been applied in a number of other studies of isotope and bulk C and water dynamics (Aranibar et al., 2006; Cooley et al., 2005; Henderson-Sellers et al., 2006; Lai et al., 2006; McDowell et al., 2008; Riley et al., 2003, 2008, 2009; Riley, 2005; Still et al., 2009; Torn et al., 2011). A brief description of the model follows to illustrate the nature of the interactions impacting δF_s. ISOLSM solves for δ_{sw} using an explicit method with boundary conditions specified for the $\delta^{18}O$ values of precipitation and above-canopy vapor. Surface evaporation is calculated in LSM1 using a laminar soil-surface boundary layer resistance and the gradient between vapor concentrations at the soil surface and canopy air. A similar approach is taken in ISOLSM to compute the soil-surface $H_2^{18}O$ flux. In this case, though, the additional effects of an equilibrium partitioning factor and a different laminar boundary layer resistance for the heavier isotopologue are included. Root water withdrawal from the soil profile (driven by transpiration) is calculated using modules from LSM1; root $H_2{}^{18}O$ withdrawal occurs

(F_s and F_s, respectively (µmol m s)) are computed from the concentration gradients and diffusivities at the soil surface. Finally, the $\delta^{18}O$ value of the soil-surface CO_2 flux is calculated as

$$\delta F_s = \left(\frac{\frac{F_s^{18}}{F_s}}{r_{\mathrm{pdb}}} - 1 \right) 1000, \tag{1}$$

where r_{pdb} is the V-PDB-CO_2 standard. As applied here, ISOLSM uses 2.5 cm control volumes to solve for δ_{sw} and twenty unevenly spaced control volumes down to 1 m depth for the soil-gas calculations. Model testing is described in Riley et al. (2003) and an application of ISOLSM to analyze the impact of near-surface δ_{sw} on δF_s is presented in Riley (2005).

2.2 High-dimensional model reduction

The HDMR technique described here (termed the cut-HDMR) is a special application of a group of tools designed to represent high-dimensional models (Alis and Rabitz, 2001; Rabitz and Alis, 1999; Rabitz et al., 1999). HDMR was developed to substantially decrease simulation runtime while retaining nonlinear interactions between state variables and model parameters. The HDMR method has been used, for example, to study global atmospheric chemistry (Wang et al., 1999), stratospheric chemistry (Shorter et al., 1999), and atmospheric radiation transport (Shorter et al., 2000).

$$g(\boldsymbol{x}) = f_0 + \sum_{i=1} f_i(x_i) + \sum_{1 \le i < j \le n} f_{ij}(x_i, x_j) + \ldots + f_{12\ldots n}(x_1, x_2, \ldots, x_n). \tag{2}$$

Here, f_0 is a constant that represents the system response at $\boldsymbol{a}$ (i.e., $g(\boldsymbol{a})$), $\boldsymbol{a}$ is the reference point (the central point of the n-dimensional hypercube defined by $\boldsymbol{x}$); $f_i(x_i)$) characterizes the impact on $g(\boldsymbol{x})$ of a change in x_i while other inputs are taken from the reference point $\boldsymbol{a}$; $f_{ij}(x_i, x_j)$ characterizes the impact on $g(\boldsymbol{x})$ of simultaneous changes in x_i and x_j; and $f_{12\ldots n}(x_1, x_2, \ldots, x_n)$ gives the residual impact on $g(\boldsymbol{x})$ of all the variables simultaneously. The cut-HDMR approach ignores functions with greater than two variable interactions under the hypothesis that first and second order interactions dominate δF_s. The three expansion functions are calculated as:

$$f_0 = g(\boldsymbol{a}), \tag{3}$$

$$f_i(x_i) = g(x_i, \boldsymbol{a}) - g(\boldsymbol{a}), \quad \text{and} \tag{4}$$

$$f_{ij}(x_i, x_j) = g(x_i, x_j, \boldsymbol{a}) - f_i(x_i) - f_j(x_j) - f_0. \tag{5}$$

The nomenclature for g indicates that it is evaluated assuming all variables are at the reference point $\boldsymbol{a}$ except the specific value(s) of x contained in the parentheses. Subtracting off the lower-order expansion functions when calculating $f_{ij}(x_i, x_j)$ ensures a unique addition from $g(x_i, x_j, \boldsymbol{a})$.

2.3 Applying HDMR to calculate δF_s

For this work the HDMR expansion functions were generated using ISOLSM to evaluate δF_s at steady state for a suite of input variables. In general, the soil-gas system will

The input variables that comprise $\boldsymbol{x}$ are assigned from a range divided into N equal intervals (Table 1). While all ISOLSM simulations here used the spatial discretizations described in Riley et al. (2002), the HDMR expansion functions are evaluated with two vertical discretization scenarios (D_1 and D_2). Scenario D_1 uses 2.5 cm soil control volumes down to 20 cm depth and N = 100, and scenario D_2 uses average soil moisture, temperature, and δ_{sw} in 5 cm increments down to 20 cm depth and N = 100.

To develop the HDMR expansion functions, ISOLSM is run to steady state for each set of conditions (i.e., each $\boldsymbol{x}$). δF_s is then evaluated and the expansion functions are calculated with Eqs. (3)–(5) and stored as look-up tables. Computing the expansion functions for each discretization took about seven days on a 2 GHz Atherton PC with 512 MB of RAM. During the HDMR simulation, first and second order interpolation routines are used to calculate the expansion functions for a specific input set $\boldsymbol{x}$. The advantage to the HDMR approach is the ability to rapidly evaluate Eq. (2) once the expansion functions have been computed.

In ISOLSM the soil CO_2 source term is calculated as the sum of autotrophic and heterotrophic respiration, each with their own exponentially decaying depth profile defined by the parameters z_0^a and z_0^h (m), respectively. z_0^a and z_0^h are sensitive to soil moisture, becoming larger as the soil dries (i.e., the soil CO_2 production moves deeper as the soil dries). To save computational time, the HDMR expansion functions were generated with a single exponential parameter, z_0. Therefore, in the simulations presented here, the HDMR model applies a parameter weighted by the predicted autotrophic, F_a ($\mu mol\, m^{-2}\, s^{-1}$), and heterotrophic, F_h ($\mu mol\, m^{-2}\, s^{-1}$), CO_2 sources to approximate the depth-distribution of CO_2 production:

The ADMR approach was tested using meteorological data from May–July 2000 in a C_4-dominated tallgrass prairie pasture in Oklahoma (36° 56′ N, 96° 41′ W). This dataset was used previously to develop and test ISOLSM (Riley et al., 2002, 2003). The site is in a region with various land uses, including crops, sparse trees, and other grasslands, has not been grazed since 1996, and is burned every spring. Maximum leaf area index is about 3 and maximum net ecosystem exchange during the growing season is about 35 μmol m^{-2} s^{-1}. The site and collection of meteorological forcing and flux data are described in detail in Suyker and Verma (2001) and Colello et al. (1998).

3 Results and discussion

The magnitude and vertical distribution of δ_{sw} is an important determinant of δF_s (Riley, 2005). In this system, low humidity, high air temperatures, and high soil evaporation rates generate strong δ_{sw} gradients in the top 5 cm of soil, making accurate prediction of δ_{sw} critical for predicting δF_s. For example, Fig. 1 shows predicted δ_{sw} for four soil layers over a twenty-day period in June 2000.

The spikes in δ_{sw} in the first soil layer occur for a number of reasons. Rapid increases in δ_{sw} are typically driven by large soil evaporative fluxes, which occur when the vapor gradient between the soil surface and canopy air is large. The δ^{18}O value of above canopy vapor (δ_v) is impacted by surface evaporative fluxes, resulting in a feedback between δ_v and near-surface δ_{sw}. Because we lack continuous measurements of δ_v, we estimate it using a constant offset (7 ‰) from the estimated stem water δ^{18}O value. In reality, δ_v can change more rapidly than this approach allows, as shown in Helliker

($\nabla_{0\text{–}5\,\mathrm{cm}}\delta_{sw}$ (‰ cm^{-1})).

Differences between ISOLSM and HDMR predictions occur for several reasons. First, discretization scenario D_2 is unable to capture the impact on δF_s resulting from large δ_{sw} gradients between 0 and 5 cm depth. We have previously shown that these gradients can substantially impact δF_s (Riley, 2005). Following precipitation (e.g., days 162, 163, 164, 167, 172, and 174; Fig. 3) the enhanced soil-surface evaporation leads to $\nabla_{0\text{–}5\,\mathrm{cm}}\delta_{sw}$ of up to 5 ‰ cm^{-1}. We have observed gradients of this magnitude in a sorghum field in Oklahoma (unpublished data), as have Miller et al. (1999) in their soil column experiments. The impact of these gradients on δF_s is better captured in scenario D_1 since this HDMR solution is based on the identical spatial discretization as that of the ISOLSM simulation (i.e., eight 2.5 cm control volumes in the top 20 cm of soil). Second, even in the absence of vertical spatial gradients in δ_{sw}, rapid changes in δ_{sw} will lead to errors in the HDMR predictions since the HDMR solution is based on the steady-state full model solution. However, the errors between the D_1 discretization scenario predictions and the ISOLSM solution are small during these periods of rapid change. These results imply that errors associated with the steady-state assumption are relatively small for the conditions simulated here. Third, using an approximation for z_0 (Eq. 6) will lead to errors in the depth distribution of CO_2 production, although the total production will be correct. Finally, the HDMR solution is linearly interpolated between the forcing values shown in Table 1; this interpolation will lead to some error. I have attempted to minimize this type of error by using relatively small increments between successive values at which the expansion functions were evaluated (i.e., $N = 100$).

the three-month period. r_c is accurately simulated by the HDMR approach for both discretization scenarios (Fig. 4). Differences in the HDMR model predictions from the full model solution during periods of large near-surface δ_{sw} gradients did not substantially impact predictions of the cumulative isoflux over the three-month period. The error in cumulative isoflux after three months is about 0.2 % (0.5 mol m^{-2} ‰) for both discretization scenarios. The HDMR solution was computed ~50 and 100 times faster than the full ISOLSM numerical solution for discretization scenarios D_1 and D_2, respectively. This increased computational efficiency makes it practical to include the ISOLSM-based HDMR solution for δF_s in regional- and global-scale models.

In the broader context, spatial heterogeneity in hydrology and biogeochemical cycling occurs on scales substantially finer than can currently, and likely ever, be directly represented in ESMs. The actual transformation of soil organic matter and CO_2 production, e.g., occurs at the 10's of nm scale, and is impacted by pore-scale heterogeneity in nutrients, water, organic molecules, mineral surfaces, microbes, and others (Kleber et al., 2011). The microbial community acting at these scales is incredibly diverse (Goldfarb et al., 2011) as are the range of organic molecules being transformed and consumed (Kogel-Knabner, 2002; Sutton and Sposito, 2005). At the mm to cm scale, aggregation, macropores, plant roots, and other soil structural properties impact distributions of microbes and resources (Six et al., 2001). Vertical structure of hydrology and C inputs can vary on horizontal scales as small as a few meters and vertical scales on the order of 10 cm. Accounting for these types of heterogeneity across 10's of km in an ESM is a substantial challenge that high-dimensional model reduction techniques such as that presented here may help address.

plex function of the depth-dependent (a) $\delta^{18}O$ value of soil water, (b) soil moisture, (c) soil temperature, and (d) soil CO_2 production, as well as the $\delta^{18}O$ value of above-surface CO_2. Mechanistic models that include these interactions (e.g., ISOLSM) may be too computationally expensive to integrate in regional and global models at their native spatial scale. The results presented here demonstrate that the HDMR technique accurately predicts δF_s up to 100 times faster than the full numerical solution.

Under rapidly changing soil moisture conditions, such as immediately after a precipitation event, the full numerical solution of the $C^{18}OO$ surface flux differs slightly from the HDMR solution. Errors in the HDMR solution arise from the steady-state assumption, approximation of the depth-dependence of soil CO_2 production, and linear interpolation. However, these errors have a small impact on the predicted cumulative isoflux. The error in the cumulative isoflux over the growing season calculated with HDMR (compared to that calculated with the full model) was less than 0.2 %.

Applying measurements of the $\delta^{18}O$ value of atmospheric CO_2 to partition measured net ecosystem fluxes into gross fluxes and, at the regional and global scale, to estimate spatially explicit CO_2 exchanges requires accurate prediction of the $\delta^{18}O$ value of the soil-surface CO_2 flux. Further, for regional and global simulations such a method must be computationally efficient. The HDMR method applied here shows great promise as a tool for addressing the need for mechanistic representation of processes across a wide range of scales and spatial heterogeneity.

Acknowledgment

DOE-LBNL work was conducted under Contract No. DE-AC02-05CH11231.

Alis, O. F. and Rabitz, H.: Efficient implementation of high dimensional model representations, J. Math. Chem., 29, 127–142, 2001.
Aranibar, J. N., Berry, J. A., Riley, W. J., Pataki, D. E., Law, B. E., and Ehleringer, J. R.: Combining meteorology, eddy fluxes, isotope measurements, and modeling to understand environmental controls of carbon isotope discrimination at the canopy scale, Glob. Change Biol., 12, 710–730, 2006.
Aubinet, M., Grelle, A., Ibrom, A., Rannik, U., Moncrieff, J., Foken, T., Kowalski, A. S., Martin, P. H., Berbigier, P., Bernhofer, C., Clement, R., Elbers, J., Granier, A., Grunwald, T., Morgenstern, K., Pilegaard, K., Rebmann, C., Snijders, W., Valentini, R., Vesala, T., and Figures, P.: Estimates of the annual net carbon and water exchange of forests: The EUROFLUX methodology, Adv. Ecol. Res., 30, 113–175, 2000
Baldocchi, D. D.: Assessing the eddy covariance technique for evaluating carbon dioxide exchange rates of ecosystems: past, present and future, Glob. Change Biol., 9, 479–492, 2003.
Baldocchi, D. D., Falge, E., Gu, L. H., Olson, R., Hollinger, D., Running, S., Anthoni, P., Bernhofer, C., Davis, K., Evans, R., Fuentes, J., Goldstein, A., Katul, G., Law, B., Lee, X. H., Malhi, Y., Meyers, T., Munger, W., Oechel, W., Paw U, K. T., Pilegaard, K., Schmid, H. P., Valentini, R., Verma, S., Vesala, T., Wilson, K., and Wofsy, S.: FLUXNET: a new tool to study the temporal and spatial variability of ecosystem-scale carbon dioxide, water vapor, and energy flux densities, B. Am. Meteorol. Soc., 82, 2415–2434, 2001.
Bonan, G. B.: A Land Surface Model (LSM version 1.0) for Ecological, Hydrological, and Atmospheric Studies: Technical Description and User's Guide, NCAR, Boulder, CO, 150 pp., 1996.
Bonan, G. B., Oleson, K. W., Vertenstein, M., Levis, S., Zeng, X. B., Dai, Y. J., Dickinson, R. E., and Yang, Z. L.: The land surface climatology of the community land model coupled to the NCAR community climate model, J. Climate, 15, 3123–3149, 2002.

Ciais, P., Tans, P. P., Denning, A. S., Francey, R. J., Troller, M., Meijer, H. A. J., White, J. W. C., Berry, J. A., Randall, D. A., Collatz, G. J., Sellers, P. J., Monfray, P., and Heimann, M.: A three-dimensional synthesis study of delta O-18 in atmospheric CO_2 2 Simulations with the TM2 transport model, J. Geophys. Res.-Atmos., 102, 5873–5883, 1997b.

Colello, G. D., Grivet, C., Sellers, P. J., and Berry, J. A.: Modeling of energy, water, and CO_2 flux in a temperate grassland ecosystem with SiB2: May–October 1987, J. Atmos. Sci., 55, 1141–1169, 1998.

Cooley, H. S., Riley, W. J., Torn, M. S., and He, Y.: Impact of agricultural practice on regional climate in a coupled land surface mesoscale model, J. Geophys. Res.-Atmos., 110, D03113, doi:10.1029/2004jd005160, 2005.

Cuntz, M., Ciais, P., Hoffmann, G., and Knorr, W.: A comprehensive global three-dimensional model of delta O-18 in atmospheric CO_2: 1. Validation of surface processes, J. Geophys. Res.-Atmos., 108, 4527, doi:10.1029/2002jd003154, 2003.

Denning, A. S., Collatz, G. J., Zhang, C. G., Randall, D. A., Berry, J. A., Sellers, P. J., Colello, G. D., and Dazlich, D. A.: Simulations of terrestrial carbon metabolism and atmospheric CO_2 in a general circulation model .1. Surface carbon fluxes, Tellus B, 48, 521–542, 1996.

Francey, R. J. and Tans, P. P.: Latitudinal variation in oxygen-18 of atmospheric CO_2, Nature, 327, 495–497, 1987.

Goldfarb, K. C., Karaoz, U., Hanson, C. A., Santee, C. A., Bradford, M. A., Treseder, K. K., Wallenstein, M. D., and Brodie, E. L.: Differential growth responses of soil bacterial taxa to carbon substrates of varying chemical recalcitrance, Front. Microbiol., 2, doi:10.3389/fmicb.2011.00094, 2011.

Goulden, M. L., Munger, J. W., Fan, S. M., Daube, B. C., and Wofsy, S. C.: Measurements of carbon sequestration by long-term eddy covariance – methods and a critical evaluation of accuracy, Glob. Change Biol., 2, 169–182, 1996.

Henderson-Sellers, A., Fischer, M., Aleinov, I., McGuffie, K., Riley, W. J., Schmidt, G. A., Sturm, K., Yoshimura, K., and Irannejad, P.: Stable water isotope simulation by current land-surface schemes: results of iPILPS phase 1, Global Planet. Change, 51, 34–58, 2006.

King, A. J., Freeman, K. R., McCormick, K. F., Lynch, R. C., Lozupone, C., Knight, R., and Schmidt, S. K.: Biogeography and habitat modelling of high-alpine bacteria, Nat. Commun., 1, doi:10.1016/J.Jconhyd.2009.12.002, 2010.

Kleber, M., Nico, P. S., Plante, A. F., Filley, T., Kramer, M., Swanston, C., and Sollins, P.: Old and stable soil organic matter is not necessarily chemically recalcitrant: implications for modeling concepts and temperature sensitivity, Glob. Change Biol., 17, 1097–1107, 2011.

Kogel-Knabner, I.: The macromolecular organic composition of plant and microbial residues as inputs to soil organic matter, Soil Biol. Biochem., 34, 139–162, 2002.

Lai, C. T., Riley, W., Owensby, C., Ham, J., Schauer, A., and Ehleringer, J. R.: Seasonal and interannual variations of carbon and oxygen isotopes of respired CO_2 in a tallgrass prairie: measurements and modeling results from 3 years with contrasting water availability, J. Geophys. Res.-Atmos., 111, D08s06, doi:10.1029/2005jd006436, 2006.

McDowell, N., Baldocchi, D., Barbour, M., Bickford, C., Cuntz, M., Hanson, D., Knohl, A., Powers, H., Rahn, T., Randerson, J., Riley, W., Still, C., Tu, K., and Walcroft, A.: Understanding the stable isotope composition of biosphere atmosphere CO_2 exchange, EOS Trans. AGU, 89, 94–95, 2008.

Miller, J. B., Yakir, D., White, J. W. C., and Tans, P. P.: Measurement of O-18/O-16 in the soil-atmosphere CO_2 flux, Global Biogeochem. Cy., 13, 761–774, 1999.

Parton, W. J., Mosier, A. R., and Schimel, D. S.: Dynamics of C, N, P, and S in grassland soils: a model, Biogeochemistry, 5, 109–131, 1988.

Peylin, P., Ciais, P., Denning, A. S., Tans, P. P., Berry, J. A., and White, J. W. C.: A 3-dimensional study of delta O-18 in atmospheric CO_2: contribution of different land ecosystems, Tellus B, 51, 642–667, 1999.

Riley, W., Still, C., Torn, M., and Berry, J.: A mechanistic model of $H_2{}^{18}O$ and $C^{18}OO$ fluxes between ecosystems and the atmosphere: model description and sensitivity analyses, Global Biogeochem. Cy., 16, 1095–1109, 2002.
Riley, W. J., Still, C. J., Helliker, B. R., Ribas-Carbo, M., and Berry, J. A.: ^{18}O composition of CO_2 and H_2O ecosystem pools and fluxes in a tallgrass prairie: simulations and comparisons to measurements, Glob. Change Biol., 9, 1567–1581, 2003.
Riley, W. J., Hsueh, D. Y., Randerson, J. T., Fischer, M. L., Hatch, J. G., Pataki, D. E., Wang, W., and Goulden, M. L.: Where do fossil fuel carbon dioxide emissions from California go? An analysis based on radiocarbon observations and an atmospheric transport model, J. Geophys. Res.-Biogeo., 113, G04002, doi:10.1029/2007jg000625, 2008.
Riley, W. J., Biraud, S. C., Torn, M. S., Fischer, M. L., Billesbach, D. P., and Berry, J. A.: Regional CO_2 and latent heat surface fluxes in the Southern Great Plains: measurements, modeling, and scaling, J. Geophys. Res.-Biogeo., 114, G04009, doi:10.1029/2009jg001003, 2009.
Shorter, J. A., Ip, P. C., and Rabitz, H. A.: An efficient chemical kinetics solver using high dimensional model representation, J. Phys. Chem., 103, 7192–7198, 1999.
Shorter, J. A., Ip, P., and Rabitz, H.: Radiation transport simulation by means of a fully equivalent operational model, Geophys. Res. Lett., 27, 3485–3488, 2000.
Six, J., Guggenberger, G., Paustian, K., Haumaier, L., Elliott, E. T., and Zech, W.: Sources and composition of soil organic matter fractions between and within soil aggregates, Eur. J. Soil. Sci., 52, 607–618, 2001.
Stern, L. A., Baisden, W. T., and Amundson, R.: Processes controlling the oxygen isotope ratio of soil CO_2: analytic and numerical modeling, Geochim. Cosmochim. Ac., 63, 799–814, 1999.
Stern, L. A., Amundson, R., and Baisden, W. T.: Influence of soils on oxygen isotope ratio of atmospheric CO_2, Global Biogeochem. Cy., 15, 753–759, 2001.

carbon dioxide in a native tallgrass prairie, Glob. Change Biol., 7, 279–289, 2001.
Tans, P. P.: Oxygen isotopic equilibrium between carbon dioxide and water in soils, Tellus B, 50, 163–178, 1998.
Tans, P. P., Fung, I., and Takahashi, T.: Observational constraints on the global atmospheric carbon dioxide budget, Science, 247, 1431–1443, 1990.
Thompson, S. E., Harman, C. J., Troch, P. A., Brooks, P. D., and Sivalpalan, M.: Spatial scale dependence of ecohydrologically mediated water balance partitioning: a synthesis framework for catchment ecohydrology, Water Resour. Res., 47, W00j03, doi:10.1029/2010wr009998, 2011.
Torn, M. S., Biraud, S. C., Still, C. J., Riley, W. J., and Berry, J. A.: Seasonal and interannual variability in C-13 composition of ecosystem carbon fluxes in the US Southern Great Plains, Tellus B, 63, 181–195, 2011.
Wang, S. W., Levy, H., Li, G., and Rabitz, H.: Fully equivalent operational models for atmospheric chemical kinetics within global chemistry-transport models, J. Geophys. Res.-Atmos., 104, 30417–30426, 1999.
Watson, R. T. and Albritton, D. L.: Intergovernmental Panel on Climate Change, Working Group I, Intergovernmental Panel on Climate Change, Working Group II, and Intergovernmental Panel on Climate Change, Working Group III: Climate Change 2001: Synthesis Report, Cambridge University Press, Cambridge, New York, 397 pp., 2001.
Wingate, L., Ogee, J., Cuntz, M., Genty, B., Reiter, I., Seibt, U., Yakir, D., Maseyk, K., Pendall, E. G., Barbour, M. M., Mortazavi, B., Burlett, R., Peylin, P., Miller, J., Mencuccini, M., Shim, J. H., Hunt, J., and Grace, J.: The impact of soil microorganisms on the global budget of delta O-18 in atmospheric CO_2, P. Natl. Acad. Sci. USA, 106, 22411–22415, 2009.
Yakir, D. and Wang, X.-F.: Fluxes of CO_2 and water between terrestrial vegetation and the atmosphere estimated from isotope measurements, Nature, 381, 515–518, 1996.

Table 1. Parameters and state variables used to generate the expansion functions. Spatial discretization scenarios D_1 and D_2 correspond to eight 2.5 cm and four 5 cm control volumes, respectively, in the top 20 cm of soil. All HDMR simulations are performed by dividing each parameter range into 100 equal spaces (i.e., $N = 100$).

Parameter or State Variable	Units	Range
soil moisture	$m^3\,m^{-3}$	0.1, 0.5
soil temperature	K	283, 303
δ_{sw}, soil water $\delta^{18}O$ value	‰ (V-SMOW)	−12, 10
$\delta^{18}O$ value of atmospheric CO_2	‰ (V-PDB)	−1, 1
soil CO_2 production	$\mu mol\,m^{-2}\,s^{-1}$	2, 8
z_0, exponential decay parameter	m	0.05, 0.2

f_0	system response at $\boldsymbol{a}$
$f_i(x_i)$	impact on $g(\boldsymbol{x})$ of a change in x_i
$f_{ij}(x_i, x_j)$	impact on $g(\boldsymbol{x})$ of simultaneous changes in x_i and x_j
$f_{12...n}(x_1, x_2, ..., x_n)$	residual impact on $g(\boldsymbol{x})$ of all the variables simultaneously
F_a, F_h	autotrophic and heterotrophic CO_2 sources (µmol m^{-2} s^{-1})
F_s^{18}, F_s	net soil-surface $C^{18}OO$ and CO_2 fluxes (µmol m^{-2} s^{-1})
$g(\boldsymbol{x})$	calculated HDMR result
I	isoflux (µmol m^{-2} s^{-1} ‰)
I_c	cumulative isoflux (mol m^{-2} ‰)
n	number of input variables in the HDMR solution
N	number of intervals in the HDMR solution for each input variable
r_{pdb}	V-PDB-CO_2 standard
$\boldsymbol{x}$	vector of variables for the HDMR solution
x_i	input variables for the HDMR solution
z_0	single exponential depth profile parameter (m)
z_0^a, z_0^h	autotrophic and heterotrophic depth profile parameters (m)
Greek letters	
δF_s	$\delta^{18}O$ value of the soil-surface CO_2 flux (‰)
δ_{sw}	$\delta^{18}O$ value of soil water (‰)
$\nabla_{0\text{–}5\,cm}\delta_{sw}$	gradient in δ_{sw} over the top 5 cm of soil (‰ cm^{-1})

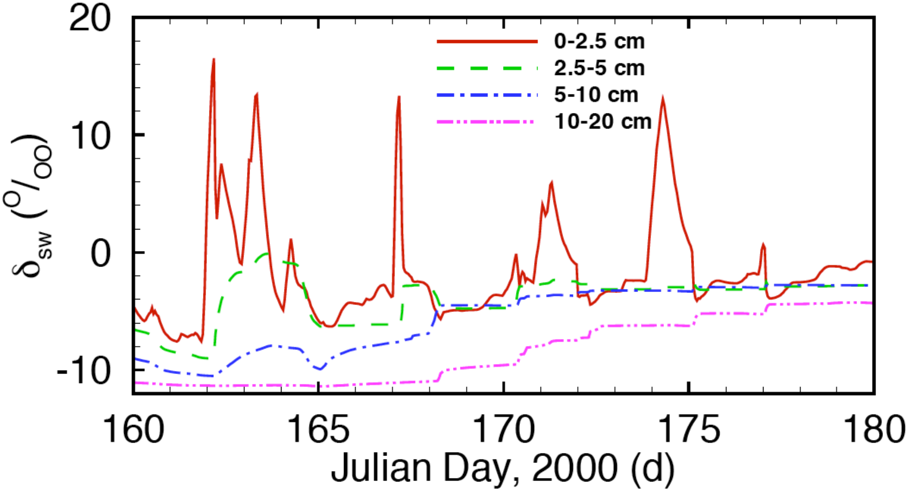

Fig. 1. Simulated δ_{sw} in four soil layers over a twenty-day period in June 2000. Spikes in δ_{sw} in the top 2.5 cm result from soil evaporation, precipitation, and wicking from lower soil layers.

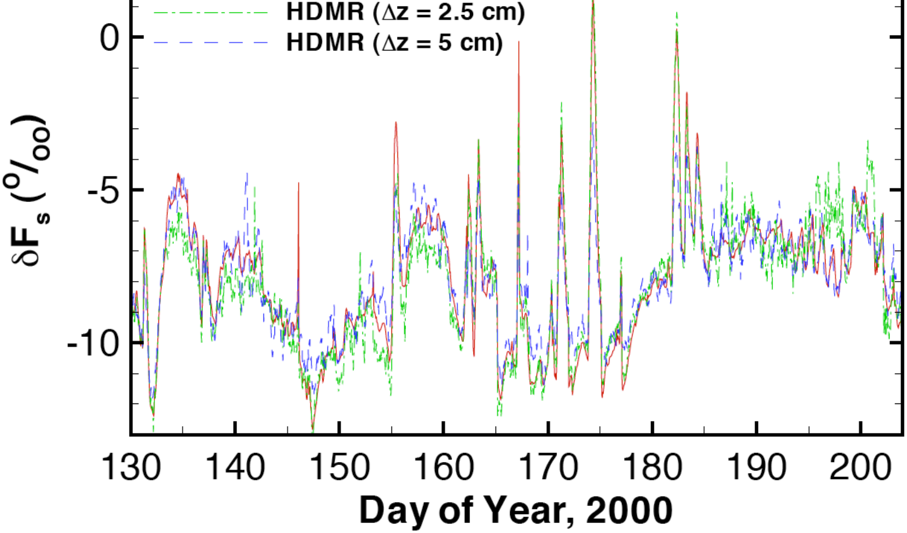

Fig. 2. Simulated δF_s over the growing season from ISOLSM and the HDMR approach using discretization scenarios D_1 and D_2. Variability in δF_s is large when δ_{sw} variability in the top 2.5 or 5 cm is large.

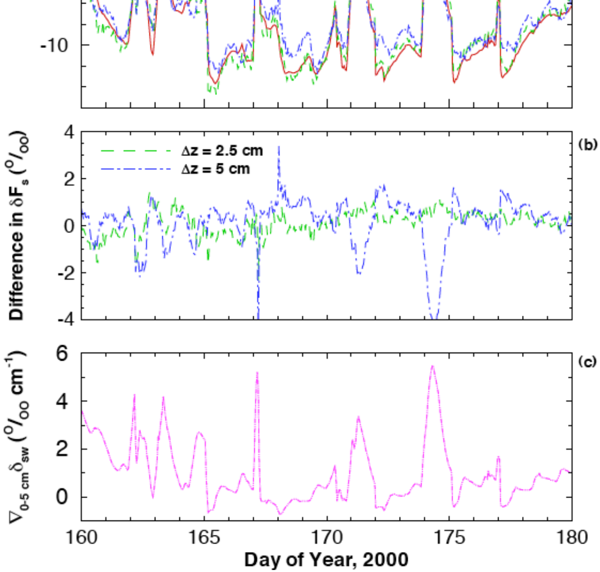

Fig. 3. (a) Same as in Fig. 2, but for a 20-day period. Also shown are **(b)** differences between the full ISOLSM model results and the HDMR predictions for Δz = 2.5 and 5 cm and **(c)** $\nabla_{0\text{–}5\,\mathrm{cm}}\delta_{\mathrm{sw}}$, the predicted gradient in δ_{sw} over the top 5 cm of soil. Differences between scenarios D_1 and D_2 are largest when near-surface δ_{sw} gradients are large. Discretization scenario D_1 more accurately predicts the impact of these gradients on δF_s since this HDMR solution is based on the identical spatial discretization as that of the ISOLSM simulation (i.e., 2.5 cm in the top 20 cm of soil).

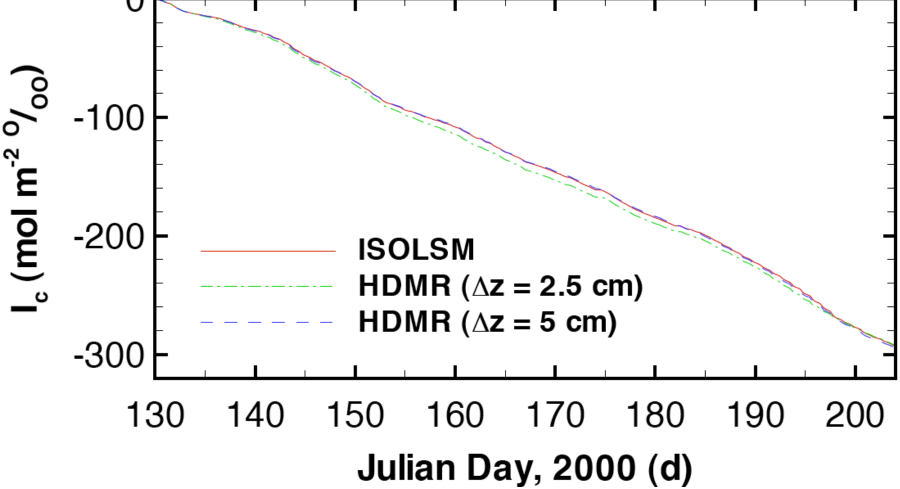

Fig. 4. Cumulative soil-surface isoflux calculated with ISOLSM and the HDMR approach using discretization scenarios D_1 and D_2. The error in cumulative isoflux over the season for each HDMR scenario is about 0.2 % (0.5 mol m^{-2} ‰).